

Features of Higher-Derivative Scalar Theories

N. Tetradis

University of Athens

- In certain higher-derivative field theories scattering can take place **at a length scale r_*** much larger than the **typical scale L_* of the nonrenormalizable terms** in the Lagrangian. (Dvali, Giudice, Gomez, Kehagias, Pirtskhalava, Grojean...)
- The center-of-mass energy can be used to define the analogue of the Schwarzschild radius: **classicalization radius r_*** .
- If all scattering takes place at $r_* \gg L_*$, the fundamental scale L_* is irrelevant and no UV completion of the theory is needed.
- I shall present a numerical study of the scenario in certain higher-derivative theories.
- Classical solutions that describe **shock fronts** may also be relevant for scattering. These solutions also describe **throats** connecting two branes.
- The effective theory of **embedded surfaces** can be used in order to reproduce the **Galileon** theory at low energies (de Rham, Tolley).
- Does this connection persist after **renormalization**?
- There is a connection with **asymptotic safety** in gravity.

Outline

- Classical evolution in field-theoretical models: quartic, DBI.
- Study of an idealized scattering process. Classicalization?
- Classical solutions of higher-derivative theories that describe surfaces embedded in Minkowski space.
- Branes with throats or shock fronts. Classicalization?
- Quantum evolution in a toy model.
- Renormalization of theories that describe surfaces. Connection with the Galileon theory and asymptotic safety.

- N. Brouzakis, J. Rizos, N. T.
arXiv:1109.6174 [hep-th] , Phys.Lett. B 708:170 (2012)
- J. Rizos, N.T.
arXiv:1112.5546 [hep-th], JHEP 1204 (2012) 110
- J. Rizos, N.T., G. Tsolias
arXiv:1206.3785 [hep-th]], JHEP 1208 (2012) 054
- J. Rizos, N.T.
arXiv:1210.4730 [hep-th], JHEP 1302 (2013) 112
- A. Codello, N.T., O. Zanusso, arXiv:1212.4073 [hep-th]
- N.T., arXiv:1212.6528 [hep-th]

Quartic model

- **Lagrangian density** ($\delta_1 = \pm 1$)

$$\mathcal{L} = \frac{1}{2} (\partial_\mu \phi)^2 - \delta_1 \frac{L_*^4}{4} \left((\partial_\mu \phi)^2 \right)^2.$$

- **Equation of motion**

$$\partial^\mu \left[\partial_\mu \phi \left(1 - \delta_1 L_*^4 (\partial_\nu \phi)^2 \right) \right] = 0.$$

- Idealized scattering process: **collapsing spherical wavepacket**

$$\phi_0(t, r) = \frac{A}{r} \exp \left[-\frac{(r+t-r_0)^2}{a^2} \right].$$

- Perturbation theory (Dvali, Pirtskhalava): strong deformation at the **classicalization radius**

$$r_* \sim L_* (A^2 L_* / a)^{1/3}.$$

- We have $r_* \gg L_*$ when the center-of-mass energy $\sqrt{s} \sim A^2/a$ is much larger than $1/L_*$.

Alternative point of view

- With spherical symmetry, the equation of motion is ($\lambda = \delta_1 L_*^4$)

$$\begin{aligned} (1 - 3\lambda\phi_t^2 + \lambda\phi_r^2) \phi_{tt} - (1 - \lambda\phi_t^2 + 3\lambda\phi_r^2) \phi_{rr} + 4\lambda\phi_r\phi_t\phi_{tr} \\ = \frac{2\phi_r}{r} (1 - \lambda\phi_t^2 + \lambda\phi_r^2). \end{aligned}$$

- This is a **quasilinear second-order partial differential equation**

$$\mathcal{A}(\phi_t, \phi_r) \phi_{tt} + \mathcal{B}(\phi_t, \phi_r) \phi_{tr} + \mathcal{C}(\phi_t, \phi_r) \phi_{rr} = \mathcal{D}(\phi_t, \phi_r, r),$$

with **discriminant**

$$\Delta = \frac{1}{4}(\mathcal{B}^2 - 4\mathcal{A}\mathcal{C}) = 3 \left(\frac{1}{3} - \lambda\phi_t^2 + \lambda\phi_r^2 \right) (1 - \lambda\phi_t^2 + \lambda\phi_r^2).$$

- $\Delta > 0$: hyperbolic, $\Delta = 0$: parabolic, $\Delta < 0$: elliptic.
- Hyperbolic equations admit wave-like solutions, while elliptic ones do not support propagating solutions.
- If \mathcal{A} , \mathcal{B} , \mathcal{C} are evaluated for the unperturbed configuration, the discriminant switches sign in the vicinity of the classicalization radius. The equation is of **mixed type**.

DBI model

- Lagrangian density

$$\mathcal{L} = -\frac{1}{\lambda} \sqrt{1 - \lambda (\partial_\mu \phi)^2},$$

- Equation of motion

$$\partial^\mu \left[\partial_\mu \phi / \sqrt{1 - \lambda (\partial_\nu \phi)^2} \right] = 0.$$

- With spherical symmetry, the equation of motion is

$$(1 + \lambda \phi_r^2) \phi_{tt} - (1 - \lambda \phi_t^2) \phi_{rr} - 2\lambda \phi_r \phi_t \phi_{tr} = \frac{2\phi_r}{r} (1 - \lambda \phi_t^2 + \lambda \phi_r^2).$$

- **Discriminant:** $\Delta = \frac{1}{4}(\mathcal{B}^2 - 4\mathcal{A}\mathcal{C}) = 1 - \lambda \phi_t^2 + \lambda \phi_r^2 \geq 0.$

- **Local energy density:** $\rho = \frac{1 + \lambda \phi_r^2}{\lambda \sqrt{1 - \lambda \phi_t^2 + \lambda \phi_r^2}} - \frac{1}{\lambda}.$

- **The total energy is conserved during the evolution.**

Possible problems

- At some stage the solution develops a **shock front**. From this point on, the numerical integration cannot be continued, as the evolution of the shock depends on additional physical assumptions about its nature (discontinuities in the field configuration, or its derivatives).
- At some time **a real solution ceases to exist** within a certain range of r . This possibility is also apparent in exact analytical solutions.
- **The equation of motion switches type** within a range of r . When it becomes elliptic, its solution requires (Dirichlet or Neumann) boundary conditions on a closed contour. The scattering problem that we are considering cannot provide such conditions, as it is set up through Cauchy boundary conditions at the initial time. Boundary conditions on a closed contour would require the values of ϕ or its derivatives at times later than the time of interest.

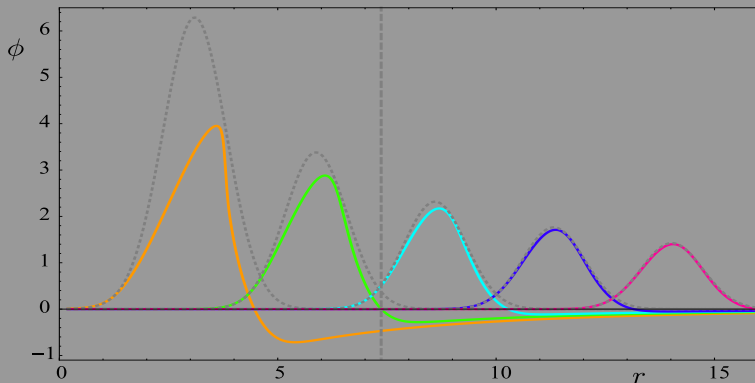


Figure: The nonlinear wavepacket at various times (solid lines) vs. the linear wavepacket (dotted lines), in the context of the **DBI model with $\lambda = 1$** . The initial wavepacket has $A = 20$, $a = 1$. The vertical dashed line denotes the classicalization radius.

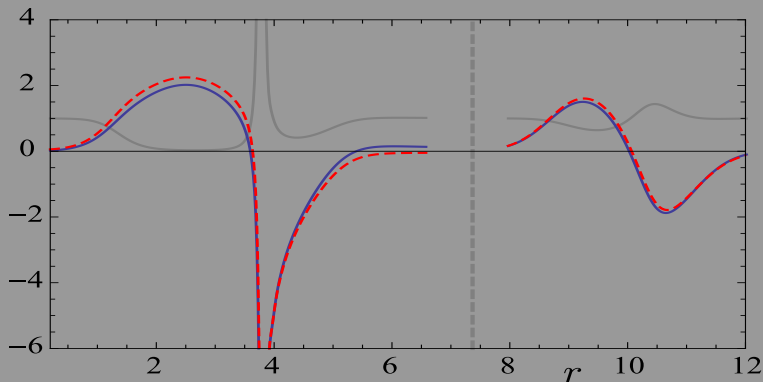


Figure: The derivatives ϕ_t (dashed) and ϕ_r (solid) of the nonlinear field, and the discriminant Δ (solid grey), at two different times, before and after the crossing of the classicalization radius. The model is the **DBI model with $\lambda = 1$** . The vertical dashed line denotes the classicalization radius.

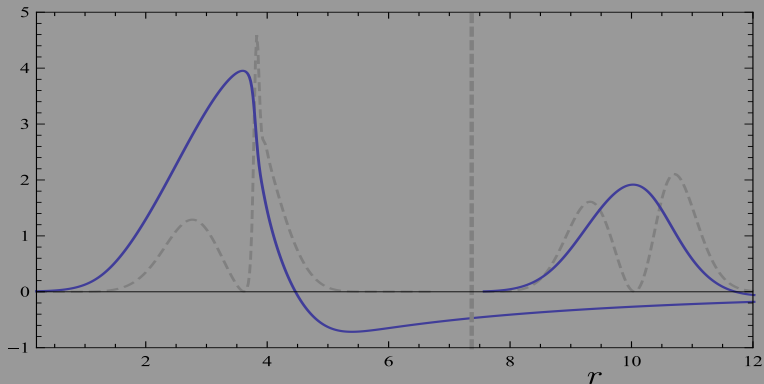


Figure: The nonlinear field ϕ (solid) and the product $4\pi r^2 \rho$, with ρ the energy density (dashed). The model is the **DBI model with $\lambda = 1$** . The vertical dashed line denotes the classicalization radius. The energy density is multiplied by 5×10^{-4} .

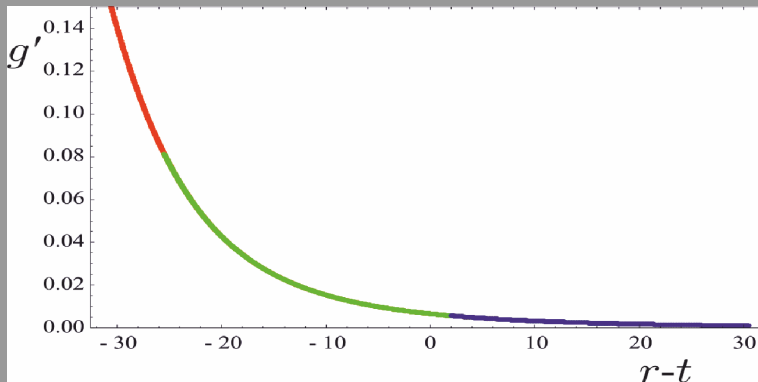


Figure: The derivative of the function $g(r - t)$ appearing in the asymptotic form $\phi(t, r) = g(r - t)/r$. A good fit can be obtained with two terms of the form $A/(r - t + c)^n$, with $n \sim 3 - 5$. The model is the **DBI model with $\lambda = 1$** .

Features

- The classicalization radius sets the scale for the onset of significant deformations of a collapsing classical configuration with large energy concentration in a central region.
- Shock fronts develop during the scattering process at distances comparable to the classicalization radius.
- An observable feature of the classical evolution is the creation of an outgoing field configuration that extends far beyond the classicalization radius. However, the scattering during the classical evolution seems to be minimal.
- Within the DBI model ($\lambda > 0$) the collapsing wavepacket can approach distances $\sim L_* = \lambda^{1/4}$ before strong scattering appears.
- Within the "wrong"-sign DBI model ($\lambda < 0$), the scattering problem may not have real solutions over the whole space. What happens in the quantum theory?

Exact analytical solutions

- Lagrangian density

$$\mathcal{L} = -\frac{1}{\lambda} \sqrt{1 - \lambda (\partial_\mu \phi)^2}.$$

- Static classicalons ($c > 0$):

$$\phi_r = \pm \frac{c}{\sqrt{r^4 - \lambda c^2}}.$$

- $\lambda < 0$: Field configuration induced by a δ -function source resulting from the concentration of energy around $r = 0$ (Dvali, Giudice, Gomez, Kehagias). Similar to **Blons** (Gibbons).
- $\lambda > 0$: The solutions have a square-root singularity at $r_s = \lambda^{1/4} c^{1/2}$. They can be joined smoothly in a continuous double-valued function of r for $r \geq r_s$: **throat connecting two $(d - 1)$ -branes embedded in $(d + 1)$ -dimensional Minkowski space**. The field ϕ corresponds to the Goldstone mode of the broken translational invariance (Gibbons).

- Exact **dynamical solutions** $\phi = \phi(z)$, with $z = r^2 - t^2$, satisfying

$$d\phi/dz = \pm \frac{1}{\sqrt{cz^4 - 4\lambda z}}.$$

- For both signs of λ , the solutions display square-root singularities at $z = 0$ and at the value z_s that satisfies $z_s^3 = 4\lambda/c$ ($c > 0$).
- For $\lambda > 0$, the singularity is located at $r_s^2 = t^2 + (4\lambda/c)^{1/3}$.
- Shock fronts** associated with meson production (Heisenberg).
- They display strong scattering at a length scale $\sim (4\lambda/c)^{1/6}$.**
- The collapsing wavepacket of the numerical analysis does not evolve into this type of solution. **The general solution is very sensitive to the initial conditions.**

Annihilating branes

- By joining solutions with opposite signs, one can create evolving networks of **throats or wormholes**, connecting two branes.
- When the throat expands, the worldvolume of the part of the branes that is eliminated reappears as energy distributed over the remaining part of the branes.
- The solutions can be generalized in the context of higher-derivative effective actions that describe surfaces embedded in Minkowski space.

Brane effective action

- Consider a **(3+1)-dimensional surface** (brane) embedded in (4+1)-dimensional Minkowski space.
- **Induced metric** in the static gauge: $g_{\mu\nu} = \eta_{\mu\nu} + \partial_\mu\pi \partial_\nu\pi$
- **Induced extrinsic curvature**: $K_{\mu\nu} = -\partial_\mu\partial_\nu\pi / \sqrt{1 + (\partial\pi)^2}$.
- Leading terms in the **effective action** (de Rham, Tolley)

$$S_\lambda = -\lambda \int d^4x \sqrt{-g} = -\lambda \int d^4x \sqrt{1 + (\partial\pi)^2}$$

$$S_K = -M_5^3 \int d^4x \sqrt{-g} K = M_5^3 \int d^4x ([\Pi] - \gamma^2[\phi])$$

$$S_R = (M_4^2/2) \int d^4x \sqrt{-g} R$$

$$= (M_4^2/2) \int d^4x \gamma ([\Pi]^2 - [\Pi^2] + 2\gamma^2([\phi^2] - [\Pi][\phi]))$$

- **Notation**: $\eta_{\mu\nu} = \text{diag}(-1, 1, 1, 1)$, $\gamma = 1/\sqrt{-g} = 1/\sqrt{1 + (\partial\pi)^2}$,
 $\Pi_{\mu\nu} = \partial_\mu\partial_\nu\pi$, square brackets represent the trace,
 $[\phi^n] \equiv \partial\pi \cdot \Pi^n \cdot \partial\pi$.

Galileon theory

- The **Galileon theory** can be obtained in the **nonrelativistic limit** $(\partial\pi)^2 \ll 1$.
- Terms involving second derivatives of the field, such as $\square\pi$, are not assumed to be small.
- The **action** becomes

$$S^{NR} = \int d^4x \left\{ -\frac{\lambda}{2}(\partial\pi)^2 + \frac{M_5^3}{2}(\partial\pi)^2\square\pi + \frac{M_4^2}{4}(\partial\pi)^2 \left((\square\pi)^2 - (\partial_\mu\partial_\nu\pi)^2 \right) \right\}$$

- Invariant under $\delta\pi = c + v_\mu x^\mu$.
- The term of highest order in the Galileon theory, omitted here, can be obtained by including in the brane action the Gibbons-Hawking-York term associated with the Gauss-Bonnet term of $(4 + 1)$ -dimensional gravity.

Equations of motion

- **Brane theory**

$$\lambda \gamma \left\{ ([\Pi] - \gamma^2 [\phi]) \right\} - M_5^3 \gamma^2 \left\{ [\Pi]^2 - [\Pi^2] + 2\gamma^2 ([\phi^2] - [\Pi][\phi]) \right\} \\ - \frac{M_4^2}{2} \gamma^3 \left\{ [\Pi]^3 + 2[\Pi^3] - 3[\Pi][\Pi^2] \right. \\ \left. + 3\gamma^2 (2([\Pi][\phi^2] - [\phi^3]) - ([\Pi]^2 - [\Pi^2])[\phi]) \right\} = 0.$$

- **Galileon theory**

$$\lambda [\Pi] - M_5^3 ([\Pi]^2 - [\Pi^2]) - \frac{M_4^2}{2} ([\Pi]^3 + 2[\Pi^3] - 3[\Pi][\Pi^2]) = 0,$$

- They have solutions of the form $\pi = \pi(r^2)$ and $\pi = \pi(z)$ with $z = r^2 - t^2$.

Solutions

- **Brane theory**

a) For $M_5 = M_4 = 0$ and $c > 0$

$$\pi_z = \pm \frac{c}{\sqrt{z^4 - 4c^2 z}}. \quad (1)$$

b) For $M_4 = 0$ and $\kappa = 12M_5^3/\lambda$

$$\pi_z = \pm \frac{\sqrt{2}c}{\sqrt{z^4 + z^3\sqrt{z^2 - 2\kappa c} - 8c^2 z - \kappa c z^2}}. \quad (2)$$

- **Galileon theory**

For $M_4 = 0$ and $\kappa = 12M_5^3/\lambda$

$$\pi_z = \frac{1}{\kappa} \left(1 - \sqrt{1 \pm \frac{2\kappa c}{z^2}} \right). \quad (3)$$

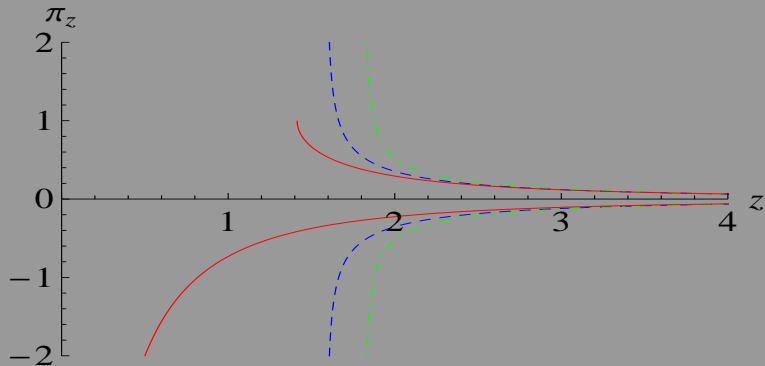


Figure: The solution $\pi_z = d\pi/dz$ for:

- The brane theory with $M_4 = M_5 = 0$ (blue).
- The brane theory with $M_4 = 0$, $12M_5^3/\lambda = 1$ (green).
- The Galileon theory with $M_4 = 0$, $12M_5^3/\lambda = 1$ (red).

- The throat solutions of the DBI theory can be generalized to solutions of the (quantum corrected) brane theory.
- The Galileon theory reproduces correctly the shape of the throats at large distances, but fails to do so at short distances.
- Similar solutions exist in the context of the **generalized Galileon theory**, and in particular in theories with **kinetic gravity braiding**.

DBI model

$$\mathcal{L} = -\frac{1}{\lambda} \sqrt{1 - \lambda (\partial_\mu \phi)^2}$$

- Momentum conjugate to the field

$$\pi = \frac{\dot{\phi}}{\sqrt{1 - \lambda \dot{\phi}^2 + \lambda (\vec{\nabla} \phi)^2}}, \quad \dot{\phi} = \pi \left[\frac{1 + \lambda (\vec{\nabla} \phi)^2}{1 + \lambda \pi^2} \right]^{1/2}.$$

A consistent classical evolution requires $1 + \lambda \pi^2 > 0$ and $1 + \lambda (\vec{\nabla} \phi)^2 > 0$ for both signs of λ .

- Hamiltonian density

$$\mathcal{H} = \frac{1}{\lambda} \left[(1 + \lambda \pi^2) \left(1 + \lambda (\vec{\nabla} \phi)^2 \right) \right]^{1/2}.$$

- The numerical integration of the equation of motion for the DBI theory with $\lambda = -1$ breaks down when $1 + \lambda \phi_r^2 = 0$ at some point in space.

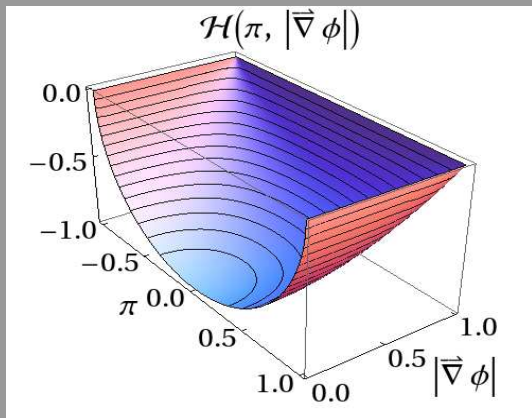


Figure: The Hamiltonian density for $\lambda = -1$, as a function of π and $|\vec{\nabla} \phi|$.

Quantum toy model

- Analogue of the DBI model ($\delta = \pm 1$)

$$L = -\frac{1}{\delta} \sqrt{1 - \delta \dot{x}^2} - \frac{1}{2} \omega^2 x^2$$

- Equation of motion: $\ddot{x} + (1 - \delta \dot{x}^2)^{3/2} \omega^2 x = 0$.
- Conserved energy: $E = \frac{1}{\delta \sqrt{1 - \delta \dot{x}^2}} + \frac{1}{2} \omega^2 x^2 = \frac{1}{\delta} + \frac{1}{2} \omega^2 x_0^2$
- $\delta = 1$: Relativistic oscillator. Analogous to DBI model with $\lambda > 0$.
- $\delta = -1$: Analogous to "wrong"-sign DBI model with $\lambda < 0$.
For $x_0^2 < 2/\omega^2$ a real oscillating solution exists.
For $x_0^2 > 2/\omega^2$ no real solution below $x^2 = x_0^2 - 2/\omega^2$, where \dot{x} diverges. **Energy cannot be conserved.**
- Similar situation in the "wrong"-sign DBI model ($\lambda < 0$) when $1 + \lambda \phi_r^2 = 0$.

- Toy model ($\delta = -1$):

Conjugate momentum: $p = \dot{x}/\sqrt{1 + \dot{x}^2}$.

It has a maximum, equal to 1, obtained for $\dot{x} \rightarrow \infty$.

- Toy model Hamiltonian: $H = -\sqrt{1 - p^2} + \frac{1}{2}\omega^2 x^2$.
- Compare with Hamiltonian density in the DBI model with $\lambda = -1$:

$$\mathcal{H} = - \left[(1 - \pi^2) \left(1 - (\vec{\nabla}\phi)^2 \right) \right]^{1/2}.$$

- Solve the Schrödinger equation in momentum space with

$$\hat{H} = -\sqrt{1 - p^2} - \frac{1}{2}\omega^2 \frac{d^2}{dp^2},$$

requiring that the wavefunction $\psi(p)$ vanishes outside the interval $[-1, 1]$.

- **Construct localized wavepackets and study their evolution in x -space.**

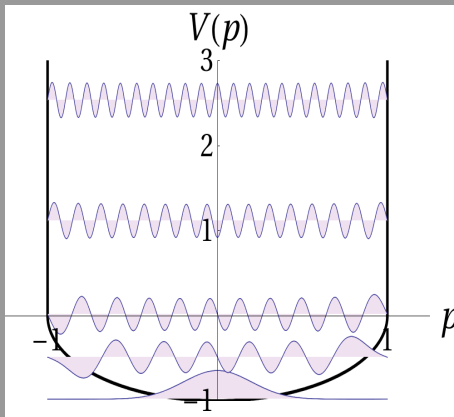


Figure: The potential for the solution of the Schrödinger equation in momentum space and the wavefunctions of several energy eigenstates.

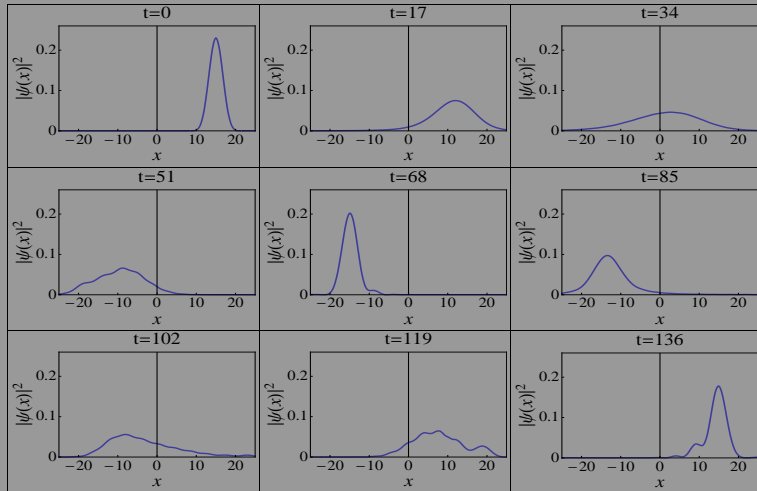


Figure: The evolution of a wavepacket initially located at $x_0 = 15$ ($\omega = 0.04$).

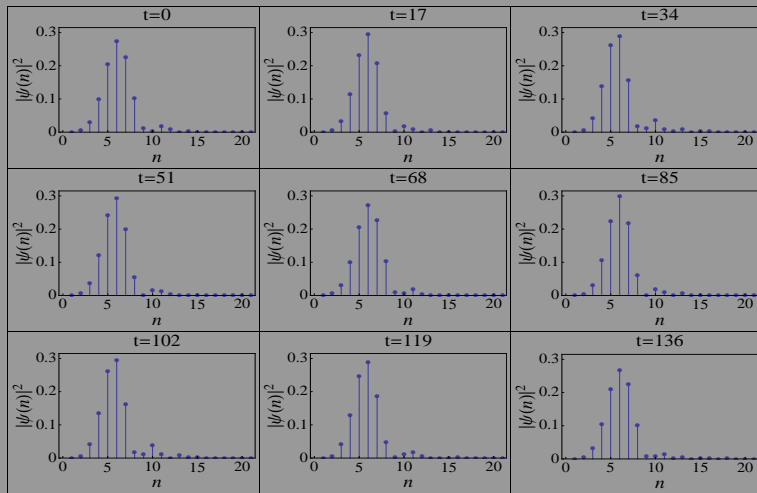


Figure: The decomposition of the wavepacket in terms of eigenstates of the harmonic oscillator.

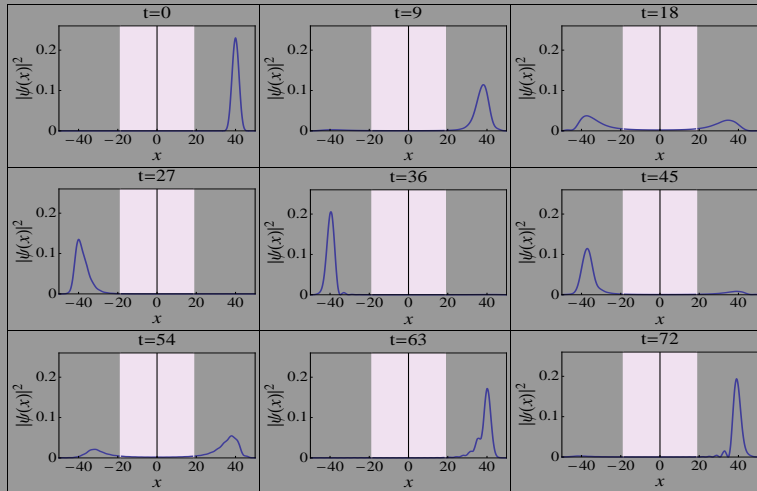


Figure: The evolution of a wavepacket initially located at $x_0 = 40$ ($\omega = 0.04$).

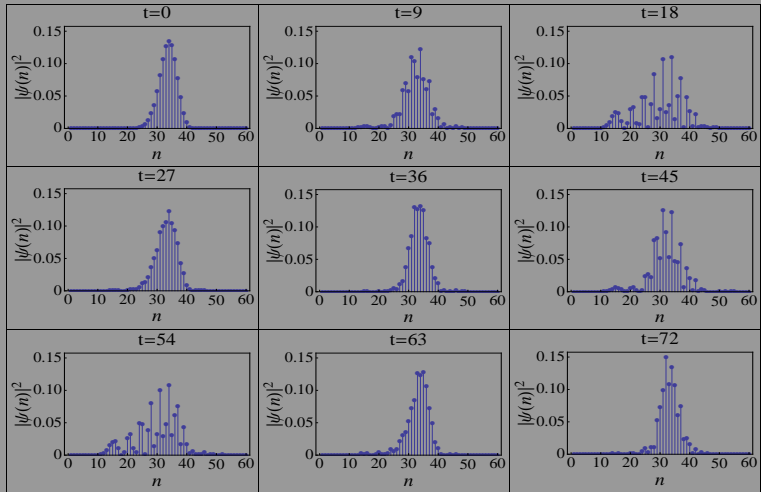


Figure: The decomposition of the wavepacket in terms of eigenstates of the harmonic oscillator.

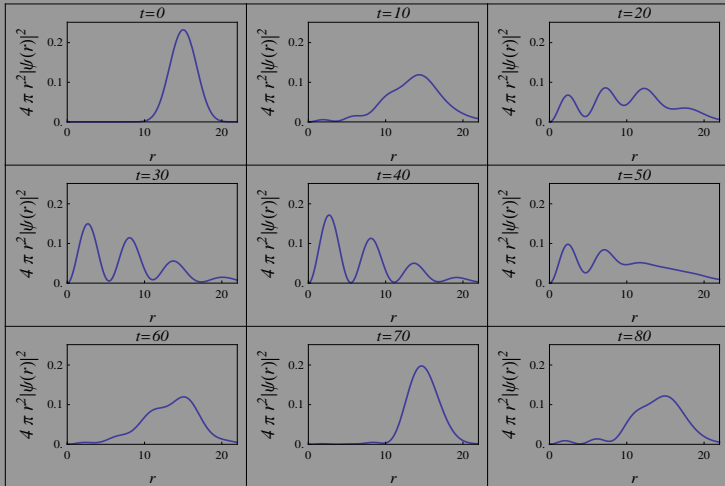


Figure: The evolution of a spherical wavepacket initially located at $r_0 = 15$ ($\omega = 0.04$).

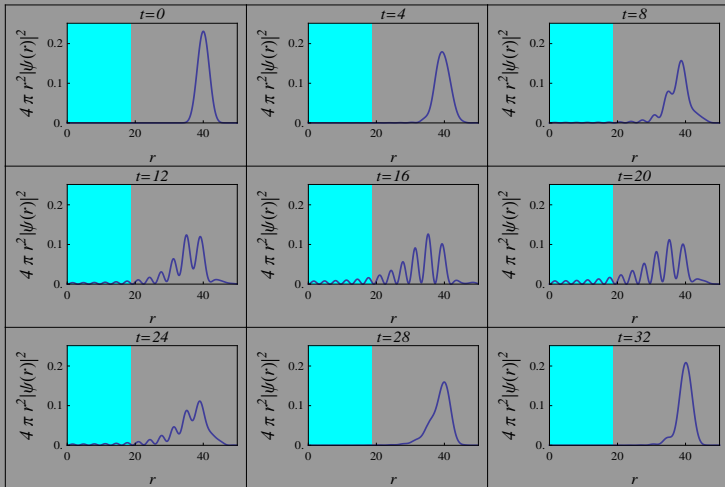


Figure: The evolution of a spherical wavepacket initially located at $r_0 = 40$ ($\omega = 0.04$).

- Theories which may lack a UV completion, such as the **"wrong"-sign DBI theory**, seem very interesting as well.
- The quantum-mechanical toy model we studied gives some hints on their properties.
- The model has a fundamental length scale and all physical states have momenta below the inverse of this scale.
- **"Scattering" within this model consists essentially of tunnelling through a region that is classically forbidden.**
- The DBI theory with $\lambda < 0$ contains **instanton-like configurations**. These are the classicalons of the Euclidean version of the theory.
- It remains to be seen how these elements can be implemented within a consistent quantum field theory.

Brane effective action

- Leading terms in the **effective action** (Euclidean space)

$$S_\lambda = \mu \int d^4x \sqrt{g} = \mu \int d^4x \sqrt{1 + (\partial\pi)^2}$$

$$S_\nu = \nu \int d^4x \sqrt{g} = -\nu \int d^4x ([\Pi] - \gamma^2[\phi])$$

$$S_\kappa = (\kappa/2) \int d^4x \sqrt{g} K^2 = (\kappa/2) \int d^4x \sqrt{g} ([\Pi] - \gamma^2[\phi])^2$$

$$S_{\bar{\kappa}} = (\bar{\kappa}/2) \int d^4x \sqrt{g} R$$

$$= (\bar{\kappa}/2) \int d^4x \gamma ([\Pi]^2 - [\Pi^2] + 2\gamma^2([\phi^2] - [\Pi][\phi]))$$

- The first Gauss-Codazzi equation gives $R = K^2 - K^{\mu\nu} K_{\mu\nu}$.
- The term S_κ becomes $\sim \pi \square^2 \pi$ in the nonrelativistic limit $(\partial\pi)^2 \ll 1$. **This term is not included in the Galileon theory.**

Renormalization

- We use the **Wilsonian (exact) renormalization group**.
- The **evolution equations** for the couplings take the form

$$\partial_t \mu_k = \frac{k^d}{(4\pi)^{d/2} \Gamma(\frac{d}{2}+1)} \frac{2\kappa_k k^2 + \mu_k}{\kappa_k k^2 + \mu_k}$$

$$\partial_t \nu_k = -\frac{k^d}{(4\pi)^{d/2} \Gamma(\frac{d}{2}+2)} \frac{d-2}{2} \frac{(2\kappa_k k^2 + \mu_k) \nu_k}{(\kappa_k k^2 + \mu_k)^2}$$

$$\partial_t \kappa_k = \frac{2k^d}{(4\pi)^{d/2} \Gamma(\frac{d}{2}+2)} \left\{ \frac{d+4}{4} \frac{(2\kappa_k k^2 + \mu_k) \kappa_k}{(\kappa_k k^2 + \mu_k)^2} + \frac{(d^2 - 2d + 4)}{d+4} \frac{(2\kappa_k k^2 + \mu_k) \nu_k^2}{(\kappa_k k^2 + \mu_k)^3} \right\}$$

$$\partial_t \bar{\kappa}_k = \frac{k^d}{(4\pi)^{d/2} \Gamma(\frac{d}{2}+2)} \left\{ \frac{d(d+2)}{12} \frac{2\kappa_k k^2 + \mu_k}{(\kappa_k k^2 + \mu_k) k^2} - \frac{16}{d+4} \frac{(2\kappa_k k^2 + \mu_k) \nu_k^2}{(\kappa_k k^2 + \mu_k)^3} \right. \\ \left. - \left[(d+2) \frac{\mu_k}{k^2} + 2d\kappa_k + \frac{3(d-2)}{2} \bar{\kappa}_k \right] \frac{2\kappa_k k^2 + \mu_k}{(\kappa_k k^2 + \mu_k)^2} \right\}.$$

- We can obtain the β -functions of $\kappa_k, \bar{\kappa}_k$ for two-dimensional fluid membranes for which the volume (now area) term is considered subleading.
- We set $d = 2, \mu_k = \nu_k = 0$ and obtain

$$\partial_t \kappa_k = \frac{3}{4\pi}, \quad \partial_t \bar{\kappa}_k = -\frac{5}{6\pi}. \quad (4)$$

- These expressions reproduce known results (Polyakov, Kleinert, Forster) for the renormalization of the **bending and Gaussian rigidities** of fluctuating membranes in a three-dimensional bulk space.
- **A nonzero value of κ is generated at the quantum level with a coefficient $\sim \nu^2$.** This corresponds to a term $\sim \nu^2 \pi \square^2 \pi$ at one loop in perturbation theory.
- The analysis of quantum corrections within the Galileon theory (Luty, Porrati, Rattazzi, Nicolis) indicates that the first correction is $\sim \nu^2 \pi \square^4 \pi$. The difference lies in the regularization scheme.

- Consider the theory with $d = 4$, $\nu = \kappa = 0$. It includes a cosmological constant and an Einstein term.
- Define the **dimensionless** cosmological and Newton's constants through

$$\frac{\mu_k}{k^4} = \frac{\Lambda_k}{8\pi G_k}, \quad \bar{\kappa}_k = -\frac{1}{8\pi G_k}. \quad (5)$$

- Their **scale dependence** is given by

$$\partial_t \Lambda_k = -2\Lambda_k + \frac{1}{6\pi} G_k (3 - 2\Lambda_k) \quad (6)$$

$$\partial_t G_k = 2G_k + \frac{1}{12\pi} \frac{G_k^2}{\Lambda_k} (3 - 4\Lambda_k). \quad (7)$$

- This system of equations has two **fixed points** at which the β -functions vanish:
 - the **Gaussian** one, at $\Lambda_k = G_k = 0$, and
 - a **nontrivial** one, at $\Lambda_k = 9/8$, $G_k = 18\pi$.
- The flow diagram is very similar to that in the scenario of **asymptotic safety**.

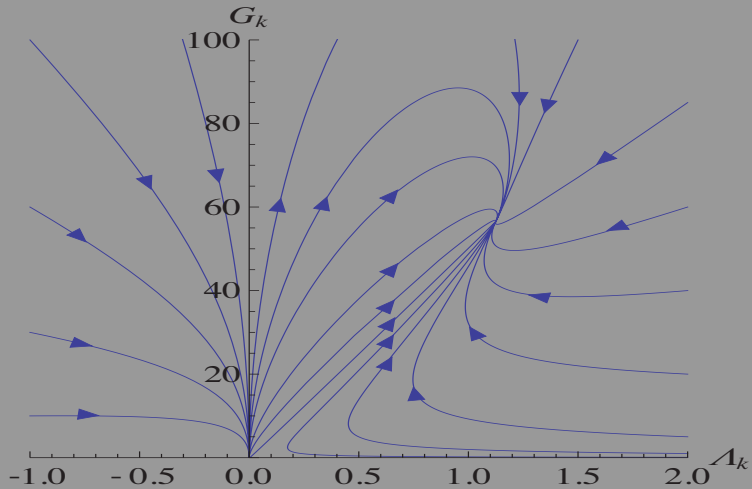


Figure: The flow diagram.